International Journal of Multidisciplinary Research and Development
Online ISSN: 2349-4182, Print ISSN: 2349-5979; Impact Factor: RJIF 5.72
Received: 04-11-2018; Accepted: 06-12-2018
www.allsubjectjournal.com
Volume 6; Issue 1; January 2019; Page No. 31-39

Projection of changes in temperature at selected meteorological stations in Zambia: statistical downscaling of CMIP5 models

Monday Chota[1*], Suman Jain[2]
[1] Ministry of General Education, Isoka, Zambia
[2] Department of Mathematics and Statistics, University of Zambia, Lusaka, Zambia

Abstract
Changes in minimum (TMIN) and maximum (TMAX) temperature over selected meteorological stations in Zambia are projected by statistically downscaling three Coupled Model Intercomparison Project Phase 5 (CMIP5) models under RCP4.5 and RCP8.5 scenarios for the period 2020 – 2049 relative to 1971 – 2000. Assessment of various predictor sets showed that a combination of sea level pressure (SLP), specific humidity at 850 hPa (Q850) and temperature at 850 hPa (T850) is suitable for downscaling TMIN while temperature at 2 metres (T2m) was found to be a predictor of choice for TMAX. Robust increase in annual and seasonal temperatures for all stations and emission scenarios is projected. Warming tends to be larger for stations located in the southern part of the country than those in the northern part. Largest seasonal warming is projected to occur during JJA under both scenarios. DJF and MAM seasons are projected to experience smallest increase in TMIN and TMAX respectively under both scenarios. Based on these results, Zambia need to devise practical adaptive strategies directed towards alleviating warming which may adversely impact health, water and agriculture sectors among others.

Keywords: CMIP5, Satistical downscaling, temperature, Zambia

1. Introduction
Global climate models (GCMs) are the main tools currently available for understanding the present and future response of the climate system of the Earth to various forcings [1] and for making climate projections for future planning [2–4]. Although GCMs are capable of simulating climate variables at global and continental scales, their outputs of coarse spatial resolution (100 – 300 km) are not suited for direct application to impact studies at local-scale where finer spatial resolution (less than 100 Km) climate and climate change information are highly sought [5–7]. Therefore, there is consensus among climate scientists that GCMs cannot resolve important localized processes of great importance to impact studies [8-10]. In view of GCMs failure to simulate local characteristics of the region of interest, they cannot be directly used to describe local climate realistically [10].

As a way of circumventing this weakness of GCMs and make them more applicable, downscaling is inevitable. Two major techniques of downscaling have been developed, namely; Dynamical and Statistical [2, 5, 8]. Dynamical downscaling (DD) involves using high resolution Regional Climate Model (RCM) driven by a low resolution GCM to represent the atmospheric physics within a limited area of interest [2]. In this way, detailed regional and local climate processes not resolved by the GCMs are captured by RCMs and high resolution climate information is generated [5]. In this technique, RCMs and the driving GCM have similar representation of physical and atmospheric dynamic processes. Therefore, it is expensive to implement DD since it requires huge computing resources and high skilled human resource like that of GCMs [2, 5, 8]. In statistical downscaling (SD), empirical relationships linking some large-scale atmospheric predictor variables to local climate variables of interest are established [5, 9, 11, 12]. The major assumption underlying SD methods is that statistical relationships remain unchanged in a changed future climate [9, 11]. Based on this assumption, these relationships are then applied to large scale variables simulated by the GCMs to produce local climate change information under different GHG emission scenarios [9, 11, 13, 14]. Thus, SD is capable of providing much needed locally relevant climate information from GCM simulations. Many studies including [15–20] have applied statistical downscaling techniques to generate high resolution climate information. However, literature suggests that downscaling of GCMs (particularly CMIP5) projections over multiple meteorological stations across Zambia has not been done [21]. Thus, adequate scientific climate change information is lacking at finer spatial resolution to empower the decision makers in formulating national policies to reduce harmful impacts of Climate Change at district and community level. Therefore, this study sought to contribute to closing up this gap by projecting changes in TMIN and TMAX at meteorological station for the period 2020 to 2049 relative to baseline 1971 to 2000 by downscaling simulations of GCMs statistically. To this aim, the study (1) investigates large-scale atmospheric variables associated with downscaling temperature over Zambia and (2) project changes in minimum temperature and maximum temperature for the period 2020 – 2049 using two emission scenarios (RCP4.5 and RCP8.5).

2. Materials and methods
2.1 Study area
In this study, temperature is downscaled at meteorological stations located across the Country. These stations are located in the three major agro-ecological regions based mainly on rainfall and soils (Fig. 1). Zambia is characterised by tropical climate with three distinguishable seasons: hot and dry season from mid-August to November, warm and wet (mid-November to April) and cool and dry (May to mid-August)

[22]. While the range of cold temperature is 3.6 ˚C to 12.0 ˚C with an average of 8.1 ˚C, hot temperature has average of 31.8 ˚C ranging from 27.7 ˚C to 36.5 ˚C [23].

Rainfall is influenced by the migration of the Inter-Tropical Convergence Zone (ITCZ) over the country. It oscillates between the northern and southern tropics over the course of a year. This phenomenon results into downward gradient of rainfall distribution from the North to the South of the country [21]. It may also lead to inter-annual variability in rainfall. The annual rainfall ranges from 700mm to 1400m in the extreme southwest and in the north respectively [23, 24] Besides ITCZ, El Niño Southern Oscillation (ENSO) has a strong influence on rainfall in Zambia as it brings about inter-annual variations. The Northern half of the country experience drier conditions in the months December – February (DJF) during La Niña episodes (cold phase) at the same time, the southern part experience wet conditions. During El Niño (warm phase) episodes, the opposite pattern occur, with the Northern half experiencing wetter conditions than normal and dry conditions in the south [24] Furthermore, northeast trade winds, southeast trade winds, northwest airflow and south airflow are the air masses that largely control the climate of Zambia.

2.2 Meteorological station data

Station data for temperature covering the period 1981 – 2010 was acquired from Zambia Meteorological Department (ZMD). Due to discontinuities in daily data, only 13 stations were utilised for minimum temperature (TMIN) and 11 for maximum temperature (TMAX) (Table 1 and Fig.1). Independent data quality control was not carried out as ZMD had already done so.

Table 1: Geographical Location of Meteorological stations used in the study

Station	Lat. (°E)	Lon.(°S)	Variable
Kabwe	14.448	28.469	Tmin
Kafironda	12.614	28.148	Tmin, Kafironda
Kasama	10.224	31.140	Tmin, Tmax
L/stone	17.823	25.820	Tmin, Tmax
LCA	15.417	28.321	Tmin, Tmax
KKIA	15.324	28.448	Tmin, Tmax
Magoye	15.998	27.617	Tmin, Tmax
Mbala	8.862	31.553	Tmin
Mongu	15.254	23.151	Tmin, Tmax
Mpika	11.901	31.433	Tmin, Tmax
Mt. Makulu	15.548	28.248	Tmin, Tmax
Ndola	12.994	28.659	Tmin, Tmax
Petauke	14.251	31.339	Tmin, Tmax

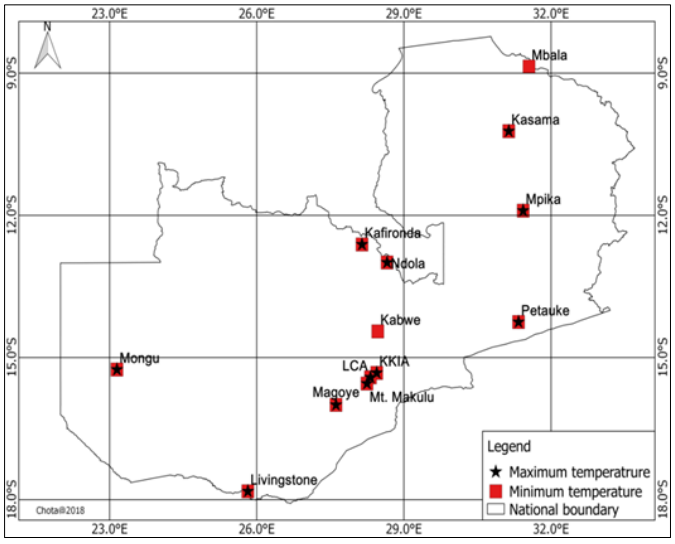

Fig 1: Spatial distribution of meteorological stations used in the study (Note: LCA means Lusaka City Airport and KKIA means Kenneth Kaunda International Airport)

2.3 Reanalysis data

Large-scale atmospheric (predictors) variables for model calibration were provided by the ERA-Interim reanalysis dataset (25) of the European Centre for Medium Range Weather Forecasts (ECMWF). This dataset runs from 1979 to date and has spatial horizontal resolution of 0.75° x 0.75°. It consists of daily estimates of both surface and atmospheric variables. This dataset is accessible at https://www.ecmwf.int/en/forecasts/datasets. Predictors considered in this study are displayed in Table 2.

Table 2: Predictor variables considered from the ERA-Interim reanalysis

Name	Code	levels (hPa*)	Units
Geopotential height	Z	1000, 850, 700, 500	m^2s^{-2}
Temperature	T	1000, 850, 700, 500	K
Specific humidity	Q	1000, 850, 700, 500	$kgkg^{-1}$
U-wind component	U	1000, 850, 700, 500	ms^{-1}
V-wind component	V	1000, 850, 700, 500	ms^{-1}
Mean sea level pressure	SLP	0	Pa
2m Temperature	T2m	0	K

2.4 Global Climate Models

Daily time series of minimum and maximum temperatures were downscaled from three GCMs of the Fifth Phase Coupled Model Intercomparison Project (CMIP5) under two concentration pathways (RCP4.5 and RCP8.5). The spatial resolution indicated for each model is for the atmospheric variables only. These models were selected based on their demonstrated ability to simulate present annual cycles of temperature and precipitation over Southern Africa [26, 27] and Zambia [21, 28].

Table 3: Global Climate Models and Scenarios used in the study

CMIP5 Model ID	Modelling centre	Atmospheric resolution	RCP
CanESM2	Canadian Centre for Climate Modelling and Analysis, Canada.	2.81° x 2.81°	RCP4.5
			RCP8.5
CNRM-CM5	National Centre for Meteorological Research, France.	1.4° x 1.4°	RCP4.
			5RCP8.5
MPI-ESM-MR	Max-Planck Institute for Meteorology, Germany.	1.875° x 1.875°	RCP4.5
			RCP8.5

2.5 Downscaling Methodology

2.5.1 Selection of geographical domain and predictors

Statistical downscaling of GCMs under perfect prognosis approach requires the screening of predictors (large-scale atmospheric variables) [10, 12] and the atmospheric domain surrounding the target region. Four geographical domains (Ds) shown in (Table 4) were assessed to determine the atmospheric window over which predictors in the ERA-Interim reanalysis (also found in GCMs) are most influential on local temperature. The geographical domains have been defined in such a way that the surrounding areas which have meteorological influence [12] on Zambia are captured. Predictors in Table 2 lead to various combinations that were tested for minimum temperature (Table 5) and maximum temperature (Table 6).

Table 4: Geographical domains considered

Code	Longitude	Latitude
D1	19 ˚E : 37 ˚E	22 ˚S : 4 ˚S
D2	19 ˚E : 37 ˚E	28 ˚S : 2 ˚N
D3	13 ˚E : 43 ˚E	22 ˚S : 4 ˚S
D4	13 ˚E : 43 ˚E	28 ˚S : 2 ˚N

Table 5: Predictor combinations tested for downscaling minimum temperature

Code	Combinations
P1	SLP, T1000, T850, Z850, T2m, Q850, Q1000, U700
P2	SLP, T850, U700, Q850, Z850
P3	SLP, T850, U700, Q850
P4	SLP, T1000, U700, Q850
P5	SLP, T850, Q850
P6	SLP, T1000, Q850
P7	SLP, T850, Q1000
P8	SLP, T2m
P9	T2m

Table 6: Predictor combinations tested for downscaling maximum temperature

Code	Combination
T1	SLP, T2m, U1000, T850, U700, Q500
T2	SLP, T2m, T850, U700, Q500
T3	SLP, T850, U700, Q500
T4	SLP, T850, U1000, Q500
T5	SLP, U1000, U700, Q500
T6	SLP, U1000, U700
T7	SLP, T850, Q500
T8	SLP, T850
T9	SLP, T2m
T10	T2m

In order to determine the most influential predictor-geographical domain combination, each predictor combination in Tables 5 – 6 was assessed over every geographical domain presented in Table 4. This resulted into 36 and 40 predictor-domain combinations for TMIN and TMAX respectively. Each of these combinations represented a possible downscaling model for the respective local climate variable. Moreover, analogue method was used to train and test each one of these combinations. Eventually, one predictor.

Geographical domain combination was finally chosen for each target local variable (TMIN and TMAX). Analogue method is based on the assumption that similar atmospheric patterns over a region of interest lead to similar meteorological outcomes [29]. Therefore, in this method, atmospheric large-scale variables are associated with local variable of interest considering observed station data [21]. The main limitation of this method consists in its inability to produce a local state that has never been observed in the historical record. In this study Euclidean distance [30] was used as a measure of similarity between the atmospheric patterns. For the purpose of predictor selection, analogue method was implemented in the perfect prognosis framework as follows: observed station dataset for the period 1981 – 2010 was divided into training period (75 percent of data: 1981 – 2002) and testing period (25 percent of data: 2003 – 2010). The training dataset was used to predict station daily time series for the testing period (2003 – 2010) using the analogue method. For this purpose, a target day t was taken from the testing period (2003 – 2010) and the analogous day u from the training period (1981 – 2002) based on the minimum Euclidean distance between the predictor combination values for day t and u. The surface variable value of the analogous day is assigned to the target day t as a predicted local-scale value. This procedure is executed for each day in the testing period to produce a predicted daily time series

$f_1, f_2, \ldots, f_n$ Where n denotes the number of days.

Each of the respective predictor combinations in Tables 5 – 6 was used to simulate predicted daily time series for each of the two local climate variables at each meteorological station. These were then compared with the corresponding daily station observation time series, from the testing period (2003 – 2010). The skill for each predictor combination was assessed based on correlation analysis and Kolmogorov Smirnov two-sample test. These measures of skill are described in section 2.5.2.

2.5.2 Validation scores

Model accuracy was checked using Pearson's correlation coefficient (rho). This measure assesses the strength and direction of linear relationship between observed (o) and simulated (f) time series. For n pairs of observations, and simulations, Pearson correlation coefficient is computed by equation Eq. (1).

$$\rho_{o,f} = \frac{\sum_{i=1}^{n}(o_i-\bar{o})(f_i-\bar{f})}{\sqrt{\sum_{i=1}^{n}(o_i-\bar{o})^2}\sqrt{\sum_{i=1}^{n}(f_i-\bar{f})^2}} \quad (1)$$

Model reliability was checked by assessing distributional similarity of the observed and simulated time series via a non-parametric two-sample Kolmogorov-Smirnov (K-S) test. The hypothesis that observed and simulated datasets come from the same distribution is tested by the K-S test using p –value approach. Very low p-values of K-S test and corresponding high K-S value implies that simulated and observed temperature time series are likely to have come from different distributions. Hence, the hypothesis must be rejected. KS test statistic is calculated using the eq. (2).

$$D = Sup_x |F_1(x) - F_2(x)| \quad (2)$$

where is the distance between cumulative density functions, and of two samples. In essence, a good downscaling model should yield higher p-values than others.

2.6 Downscaling GCMs Scenarios

After selecting the downscaling model using station daily data and ERA-Interim, the analogue method was again used to simulate daily future and baseline values of local variables. For the purpose of downscaling GCM simulations, the model built was applied to GCMs. In this case, the large-scale atmospheric variable from the GCM for a targeted day t (within downscaling period) was compared to large scale variables in the reanalysis record (1981 – 2010) using Euclidean distance as a measure of similarity. The surface estimate in the reanalysis record corresponding to the analogue is the downscaled value for day t. Studies that have used analogue method to downscale temperature include [7, 31]. This procedure was implemented using a web based statistical downscaling portal accessed on https://www.meteo.unican.es/downscaling/ensembles to downscale daily time series for minimum temperature and maximum temperature for baseline period (B) (1971 – 2000) and future period (F) (2020 – 2049) at weather station level from three GCMs constrained by two representative concentration pathways: RCP4.5 and RCP8.5.

2.7 Computation of climate change signal and analysis of scenarios

The climate change signal was computed using delta method. In this method, the change in climate is computed by subtracting mean of the baseline period from the mean of the future period. Equation 3 was used to compute the climate change signal for temperature.

$$\Delta_T = \bar{Y}_F - \bar{Y}_B \quad (3)$$

where Δ_T = change in temperature and

$$\bar{Y}_i = \begin{cases} \text{mean of future period, if i} = F \\ \text{mean of baseline period, if i} = B. \end{cases}$$

In this paper, results for projected changes in minimum and maximum temperature are reported using the ensemble mean of models for each RCP. The use of ensemble mean is very common in climate change studies [32, 33]. It is one way of reducing uncertainty associated with model configuration. Furthermore, the use of more than one scenario offers an opportunity to look at a range of plausible future climate change [34]. Studies such as [1, 33, 35, 36] show that model ensemble results are better than those of any single GCM. This is attributed to the presence of information from all participating models and single models tend to be overconfident. Uncertainty in the projected mean climate change is expressed quantitatively using model spread (a range of values calculated by various models). IPCC have used model spread as a measure of uncertainty of climate change projections in a number of their reports. Robustness of the projected changes was ensured by computing ensemble mean of at least two GCMs with the same sign of change. This is one of the methods for determining the robustness of a climate change signal [37] and it has been applied in other studies.

3 Results and discussion

3.1 Predictors for Minimum Temperature

Pearson correlation coefficients (rho) for each predictor for minimum temperature (Tmin) are generally high over each domain (Figure 8a). With exception of predictor combinations P8 (SLP, T2m) and P9 (T2m), Pearson correlation coefficient (rho) is largest over the smallest domain D1 for most predictor combinations (P1 – P7). In the case of KS-p values (figure 8b), D1 consistently yielded highest values of rho for each predictor combination. Thus, the smallest domain, D1 was selected for downscaling minimum temperature since it yielded better correlations and KS-p values compared to other domains. This is consistent with [10] whose findings show that analogue method performs better over smaller domain. Comparing the performance of predictors over D1, excluding P8 and P9 based on their low correlation coefficients, results show that predictor combination P1 has the largest correlation coefficient but lowest KS-p value over the domain of choice D1.

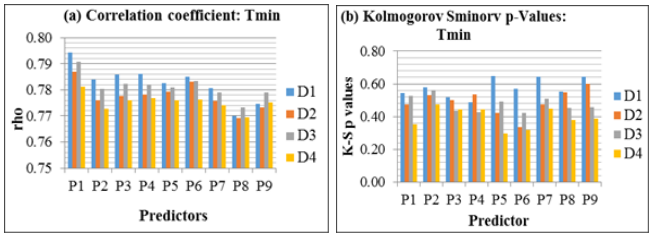

Fig 2: Validation measures for minimum

Temperature

Although P1 is highly correlated with Tmin (r = 0.79) than any other combination, it was not a preferred predictor choice owing to its low KS-p value (0.54) and many large-scale variables. Discarding P1 based on the large number of variables combined is in agreement with [38] who warned against using excessive number of predictors as this may lead to multi-collinearity and poor prediction accuracy.

Other predictors with comparable rho over D1 are P2 (0.784), P3 (0.786), P4 (0.786), P5 (0.783), P6 (0.785) and P7 (0.781). Comparing their KS- p values over D1, results show that P5 and P7 out performs them all with respective KS- p values of 0.647 and 0.644. Based on correlation coefficient and KS- p values P5 (SLP, T850, Q850) is a predictor set of choice for downscaling minimum temperature. Results also show that exclusion of circulation variables as in predictor sets P5 to P9 leads to larger p-values of Kolmogorov Smirnov test. This implies improved distribution similarity between observed and downscaled time series for minimum temperature. This is desirable under climate change conditions and consistent with [10] who established that temperature and/or humidity

variables tend to have stronger climate change signal than zonal and meridional wind component in the case of temperature.

3.2. Predictors for Maximum Temperature

Figure 3 display validation scores: rho (panel a) and KS-p values (panel b) for maximum temperature. Similar to precipitation and minimum temperature, the smallest domain (D1) yields better correlations for all predictor combinations (Figure 3a). This is evident through higher correlation values for all predictor sets over D1. Moreover, with exception of predictor sets T6 (SLP, U1000, U700) and T10 (T2m) whose KS-p values are 0.678 and 0.618 respectively, other predictor sets have low p-values of Kolmogorov Smirnov test (Figure 3b). However, T10 composed of T2m only had a better correlation coefficient (rho = 0.757) than T6 which is composed of circulation variables only and had the smallest correlation coefficient (rho = 0.716). Moreover, the removal of temperature variables from the predictor field as it is the case with combinations T5 (SLP, U1000, U700, Q500) and T6 (SLP, U1000, U700) lead to the decrease in correlation coefficient. Thus inclusion of temperature variables improves predictive power of the downscaling model for Tmax and Tmin. This result is in agreement with findings of earlier studies that established that circulation variables only tend have weaker climate signal [10]. The use of T2m in place of T850 marginally reduces correlation coefficient from 0.763 to 0.758 but increases KS-p value from 0.484 to 0.495. The implication of this is that T2m improve distribution similarity and hence model reliability. This is desirable under climate change conditions. Although the predictor set T7 (SLP, T850, Q500) exhibit high correlations, it has low p values of K-S test.

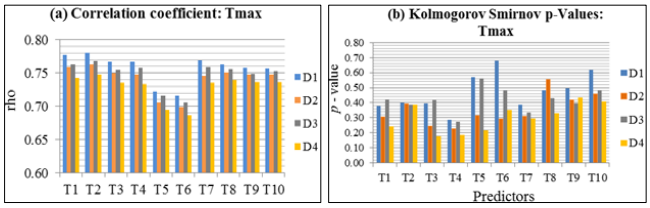

Fig 3: Validation measures for Maximum

Temperature (Tmax)

Removing Q500 from T7 slightly reduced correlation coefficient but increased KS-p value for Tmax. The implication of this is that upper tropospheric variables improve distributional similarity of observed and downscaled time series for Tmax. Therefore, predictor set T10 (T2m) is preferred for downscaling Tmax since it yielded comparably high correlation and KS-p values over D1 [18]. used the same predictor for downscaling temperature in Russia and Norway.

3.3. Projected Temperature

3.3.1 Mean annual minimum temperature and maximum temperature

The ensemble of models consistently indicates increase in mean annual minimum temperature (Fig. 4a) and mean annual maximum temperature (Fig. 4b) across all stations and representative concentration pathways. These results are in harmony with earlier studies [22, 39, 40] which projected increase in temperature for Zambia. Conforming to the findings of [41, 42], the annual mean minimum temperature and annual mean maximum temperature are projected to be higher under RCP8.5 than RCP4.5 for all stations. The largest minimum temperature of 17.8°C and 17.9°C under RCP4.5 and RCP8.5 respectively is projected to be experienced over Petauke. Moreover, the smallest minimum temperature of 12.0°C and 12.2°C under the two respective scenarios is projected over Kafironda. Mpika meteorological station is projected to experience the lowest annual mean maximum temperature under both RCPs, with 27.9°C and 28.2°C for RCP 4.5 and RCP 8.5 respectively (fig. 4b). The largest annual mean maximum temperature differs depending on station and RCP. Under RCP4.5, the largest value of 32.2°C is projected to occur over Livingstone while the largest value of 32.4°C under RCP8.5 is expected over Mongu and Livingstone.

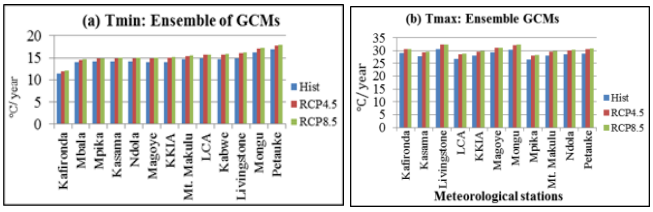

Fig 4: Downscaled projections of annual mean TMIN (panel a) and TMAX (panel b) for the control (1971 – 2000) and future (2020 – 2049) time periods using ensemble of models.

3.3.2 Projected changes in annual mean minimum temperatures

Figures 5 – 6 show projections of changes in minimum temperature using the ensemble of models under the two scenarios. The ensemble average of three GCMs projects increase in minimum temperature over every station. Livingstone will very likely experience the largest increase of 1.15°C and 1.32°C under RCP4.5 and RCP8.5 respectively. Least increase of 0.59°C and 0.69°C projected over Mbala under the two scenarios. Projected warming tends to be higher towards the southern part of the country than northern half under both emission scenarios. Figures 5 – 6 indicate that minimum temperature is projected to increase by 0.59 – 1.32°C across meteorological stations regardless of the emission scenario considered.

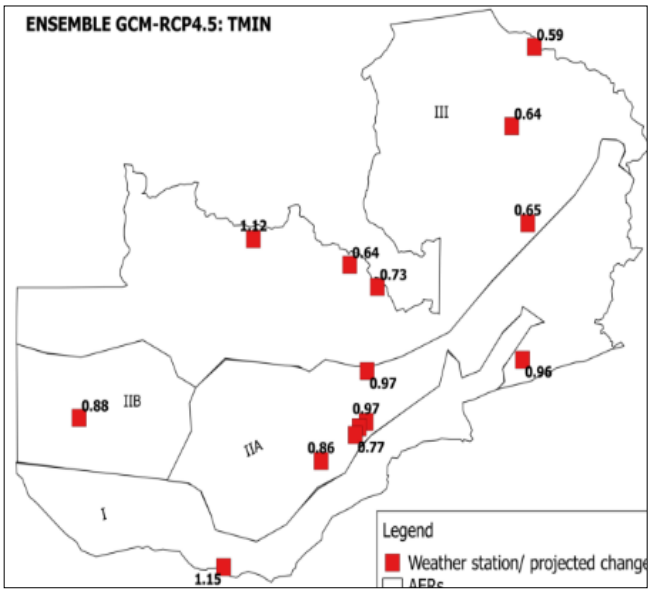

Fig 5: Projected changes in downscaled mean annual TMIN for ensemble of GCMs under RCP4.5 scenario for the period 2020 – 2049 relative to 1971 – 2000.

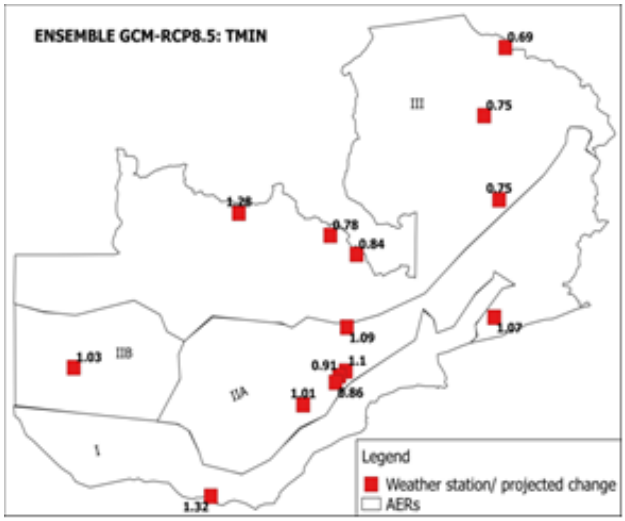

Fig 6: Projected changes in downscaled mean TMIN for ensemble of GCMs under RCP8.5 scenario for the period 2020 – 2049 relative to 1971 – 2000.

3.3.3 Projected changes in maximum temperature

The ensemble mean of three GCMs projects increase in maximum temperature over every station and two emission scenarios. Petauke will very likely experience the largest increase of 1.85°C and 2.08°C under RCP4.5 and RCP8.5 respectively. Least increase of 1.45°C and 1.63°C projected over Kafironda under the two scenarios. Like minimum temperature, changes in maximum temperature tend to get larger towards the southern part of the country under both emission scenarios projects increases (Figs. 7 and 8).

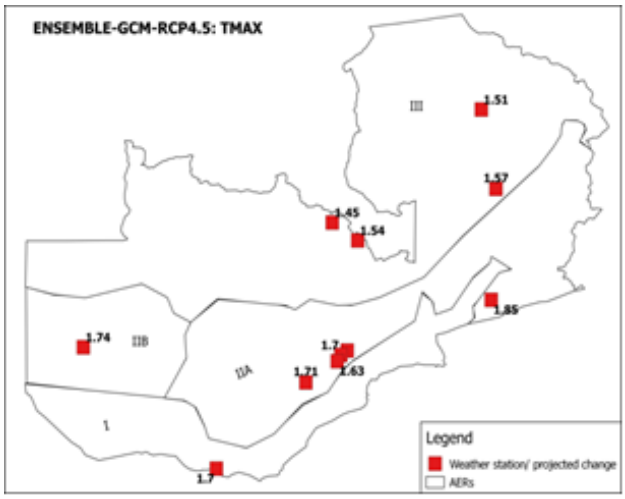

Fig 7: Projected changes in downscaled mean annual TMAX for ensemble of GCMs under RCP4.5 scenario for the period 2020 – 2049 relative to 1971 – 2000.

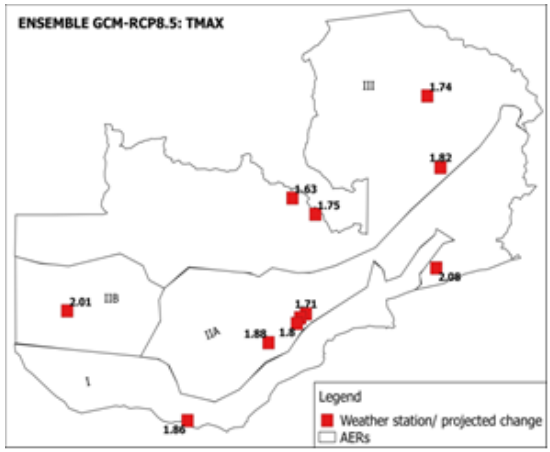

Fig 8: Projected changes of downscaled TMAX from the ensemble of three GCMs under RCP 8.5 scenario for the period 2020 – 2049 relative to 1971 – 2000.

3.3.4 Projected Seasonal Temperature Changes

On seasonal basis, the ensemble of models projects increase in both minimum temperature and maximum temperature for all seasons and all weather stations under the two emission scenarios. The increase gets bigger with the increase in concentration of emissions (Figs. 9 – 10). Thus, changes are bigger under RCP8.5 than RCP4.5 for most stations. For minimum temperature, largest and smallest increases at each station are projected to occur during JJA and DJF seasons respectively under the two future scenarios (Fig. 9).

The Ensemble of models show that for DJF season, Kafironda will experience the smallest increase of 0.26°C and 0.29°C in mean minimum temperature under RCP4.5 and RCP8.5 respectively. Similarly, Mbala is projected to experience the smallest rise in mean minimum temperature of 0.47°C (RCP4.5) and 0.57°C (RCP8.5) during MAM season, 1.04°C (RCP4.5) and 1.21°C (RCP8.5) in JJA, and 0.38°C (RCP4.5) and 0.42°C (RCP8.5) for SON (Fig. 9). Apart from JJA season under RCP4.5, Livingstone is consistently projected to experience the highest increase for DJF, MAM and SON seasons and under both scenarios. For RCP4.5, seasonal mean minimum temperature for Livingstone will rise by 0.68°C (DJF), 1.25°C (MAM) and 1.30°C (SON). For JJA season the largest increase of 1.41°C is projected to occur over Kabwe station (Fig. 9a). As for RCP8.5, the ensemble of models projects increases of 0.74°C (DJF), 1.50°C (MAM), 1.68°C (JJA) and 1.35°C (SON) in minimum temperature for 2020 – 2049 relative to 1971 – 2000 (Fig.9b). Livingstone is projected to have the largest increase in minimum temperature in all seasons (SON, DJF, MAM, and JJA). This can have implications on tourism sector in the tourist capital.

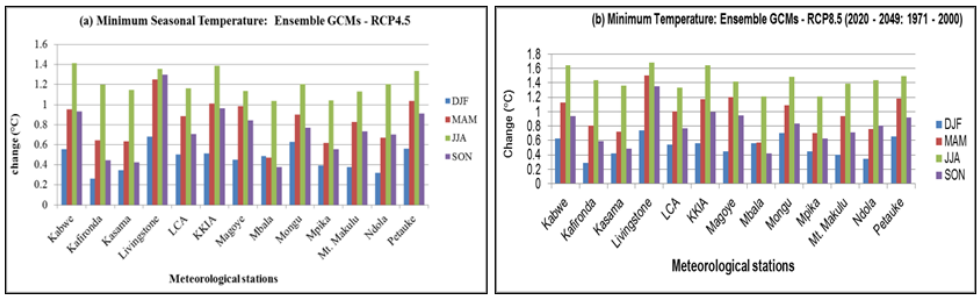

Fig 9: Projected changes of downscaled seasonal minimum temperature using the ensemble of three GCMs under RCP4.5 and RCP 8.5 emission scenarios for the period 2020 – 2049 relative to 1971 – 2000.

The Ensemble of models projects seasonal mean maximum temperature to increase by 1.45 – 1.85°C (DJF), 1.37 – 1.84°C (MAM), 1.56 – 2.07°C (JJA) and 1.35 – 1.86°C (SON) under RCP4.5 emission scenario (Fig. 10a). Largest warming is projected to occur during JJA season for all weather stations under RCP4.5 and only most stations for RCP8.5 (Fig. 10). Moreover, the increase in seasonal maximum temperature under RCP8.5 is projected to be in the range of between 1.59 and 2.22°C (DJF), 1.49 and 2.21°C (MAM), 1.73 and 2.39°C (JJA) and 1.35 and 1.95°C (SON) (Fig. 10b). Results show that changes in temperature tend to get larger towards southern part of the country.

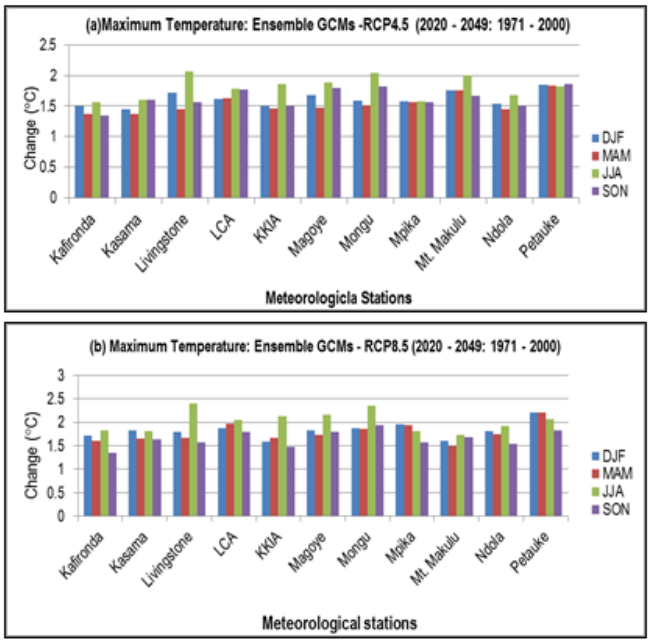

Fig 10: Projected changes of downscaled seasonal maximum temperature using the ensemble of three GCMs under RCP4.5 (panel a) and RCP 8.5 (panel b) emission scenarios for the period 2020 – 2049 relative to 1971 – 2000.

In agreement with previous studies [22, 39] the current study has projected increase in annual and seasonal temperature across all meteorological stations for both emission scenarios. This robust indication of direction of changes in both minimum and maximum temperatures can be seen in Figs 4 – 10. Warming for Zambia is projected to be much less than 4°C the projected warming for southern Africa (43) and tend to be larger towards the southern region. Zambia is characterised by relatively high temperatures with potential evapo-transpiration larger than precipitation [22]. Thus, continued increase in temperature may exacerbate adverse impacts of climate change on water resources and agriculture sector which is mainly rainfall dependent [44].

Conclusions

This study projected changes in minimum and maximum temperature for the period 2020 – 2049 relative to 1971 – 2000 using three CMIP5 GCMs under RCP4.5 and RCP8.5 scenarios over selected meteorological stations in Zambia. The study focused on the annual and seasonal temporal scales. Assessment of different combinations of large-scale atmospheric variables showed that predictor set consisting Sea level pressure, air temperature at 850 hPa and specific humidity at 850 hPa is suitable for downscaling minimum temperature. In the case of maximum temperature, temperature at 2 meters (T2m) was the preferred predictor choice.

The study has projected robust increase in minimum temperature and maximum temperature for all stations and emission scenarios. Analysis of projected changes in minimum and maximum surface temperature over selected meteorological stations shows that warming tends to be larger for stations located in the southern part of the country than those in the northern part. The magnitude of warming increases from northern part to southern part. Regardless of the emission scenario considered, minimum temperature for the period 2020 – 2049 is projected to increase by 0.59 – 1.32°C across meteorological stations relative to the baseline 1971 – 2000. Furthermore, maximum temperature is projected to increase by 1.45°C – 2.08°C across meteorological stations regardless of the emission scenario.

On a seasonal scale, temperature is projected to increase across all stations during each season. Smallest increase in minimum temperature is projected to occur during DJF season with JJA expected to experience largest increase for every station under both emission scenarios. In the case of maximum temperature, smallest increase is projected to occur during MAM season for most stations. Besides, largest increases are projected for JJA season under both emission scenarios for the majority of stations.

Results seem to suggest that the Zambia need to devise practical adaptive strategies and policies directed towards alleviating impacts of global warming. Projected warming may impact health, water and agriculture sectors.

5. Acknowledgements

Authors wish to acknowledge the Santander Meteorology Group of University of Cantabria for the provision of the ENSEMBLES Downscaling Portal used in statistical downscaling.

6. Conflict of Interest

No competing interests exist

7. References

1. Flato G, Marotzke J, Abiodun B, Braconnot P, Chou SC, Collins W, *et al.* Evaluation of Climate Models. Clim Chang 2013 Phys Sci Basis Contrib Work Gr I to Fifth Assess Rep Intergov Panel Clim Chang. 2013; pp. 741-866.
2. Maraun D, Wetterhall F, Chandler RE, Kendon EJ, Widmann M, Brienen S, *et al.* Precipitation downscaling under climate change: Recent developements to bridge the gap between dynamical models and the end user. Rev Geophys. 2010; 48(2009RG000314):1-38.
3. Osman Y, Al-Ansari N, Abdellatif M, Aljawad SB, Knutsson S. Expected Future Precipitation in Central Iraq Using LARS-WG Stochastic Weather Generator. Engineering. 2014; 06(13):948-59.
4. Grose MR, Bhend J, Argueso D, Ekström M, Dowdy AJ, Hoffmann P, *et al.* Comparison of various climate change projections of eastern Australian rainfall. Aust Meteorol Oceanogr J. 2015; 65(1):72-89.
5. Trzaska S, Schnarr E. A review of downscaling methods for climate change projections. United States Agency Int Dev by Tetra Tech ARD. 2014; September:1-42.
6. Benestad R. Downscaling Climate Information Downscaling Climate Information Summary and Keywords. In: Oxford Research Encyclopedia of

Climate Science. 2016; pp. 1-37.
7. Grouillet B, Ruelland D, Ayar PV, Vrac M. Sensitivity analysis of runoff modeling to statistical downscaling models in the western Mediterranean. Hydrol Earth Syst Sci. 2016; 20(3):1031-47.
8. Hewitson B, Crane R. Climate downscaling: techniques and application. Clim Res. 1996; 7:85-95.
9. Wilby RL, Charles SP, Zorita E, Timbal B, Whetton P, Mearns LO. Guidelines for Use of Climate Scenarios Developed from Statistical Downscaling Methods. Analysis. 2004; 27(August):1-27.
10. Gutiérrez JM, San-Martín D, Brands S, Manzanas R, Herrera S. Reassessing statistical downscaling techniques for their robust application under climate change conditions. J Clim. 2013; 26(1):171-88.
11. Von Storch H, Hewitson B, Mearns L. Review of Emperical Downscaling Techniques. In: Iversen T, Hoiskar BA., editors. Regional climate development under global warming General Technical Report. Torbjornrud: Conference Proceedings RegClim Spring Meeting. 2000; pp. 29-46.
12. Ribalaygua J, Pino MR, Pórtoles J, Roldán E, Gaitán E, Chinarro D, *et al*. Climate change scenarios for temperature and precipitation in. Sci Total Environ. 2013; 464(1):1015-30.
13. Evans JP. CORDEX – An international climate downscaling initiative. 19th Int Congr Model Simul. 2011; 10:12-6.
14. Hewitson BC, Daron J, Crane RG, Zermoglio MF, Jack C. Interrogating empirical-statistical downscaling. Clim Change. 2014; 122(4):539-54.
15. Huth R. Statistical downscaling in central Europe: Evaluation of methods and potential predictors. Clim Res. 1999; 13(2):91-101.
16. Hewitson BC, Crane RG. Consensus between GCM climate change projections with empirical downscaling: Precipitation downscaling over South Africa. Int J Climatol. 2006; 26(10):1315-37.
17. Wetterhall F, Halldin S, Xu CY. Statistical precipitation downscaling in central Sweden with the analogue method. J Hydrol. 2005; 306(1-4):174-90.
18. Benestad RE. Empirical-Statistical Downscaling of Russian and Norwegian temperature series. 2008; 13.
19. Luo Q, Wen L, McGregor JL, Timbal B. A comparison of downscaling techniques in the projection of local climate change and wheat yields. Clim Change. 2013; 120(1-2):249-61.
20. Chisanga C, Phiri E, Chisanga CB, Phiri E, Chinene VRN. Statistical Downscaling of Precipitation and Temperature Using Long Ashton Research Station Weather Generator in Zambia: A Case of Mount Agriculture Research Station. Am J Clim Chang. 2017; 6(August):487-512.
21. Libanda B, Allan D, Noel B, Luo W, Chilekana N, Nyasa L. Predictor Selection Associated With Statistical Downscaling of Precipitation over Zambia. Asian J Phys Chem Sci. 2016; 1(2):1-9.
22. NAPA. Formulation of the National Adaptation Programme of Action on Climate Change (Final Report). Lusaka, Zambia; 2007.
23. Kasali G. Capacity Strengthening in the Least Developed Countries(LDCs) for Adaptation to Climate Change (CLACC): Climate Change and Health in Zambia, 2008.
24. Kanyanga JK. EL NIÑO Southern Oscillation (ENSO) and Atmospheric Transport over Southern Africa. 2008. PhD Thesis. University of Johannesburg. South Africa.
25. Dee DP, Uppala SM, Simmons AJ, Berrisford P, Poli P, Kobayashi S, *et al*. The ERA-Interim reanalysis: Configuration and performance of the data assimilation system. Q J R Meteorol Soc. 2011; 137(656):553-97.
26. McSweeney CF, Jones RG, Lee RW, Rowell DP. Selecting CMIP5 GCMs for downscaling over multiple regions. Clim Dyn. 2015; 44(11-12):3237-60.
27. Munday C, Washington R. Circulation controls on southern African precipitation in coupled models: The role of the Angola Low. J Geophys Res Atmos. 2017; 122(122):861-77.
28. Chisanga CB, Phiri E, Chinene VRN. Statistical Bias Correction of Fifth Coupled Model Intercomparison Project Data from the CGIAR Research Program on Climate Change, Agriculture and Food Security - Climate Portal for Mount Makulu, Zambia. Br J Appl Sci Technol. 2017; 21(4):1-16.
29. Manzanas RG. Statistical Downscaling of Precipitation in Seasonal Forecasting : Advantages and Limitations of Different Approaches. 2016; PhD Thesis. University of Cantabria; Spain.
30. Matulla C, Zhang X, Wang XL, Wang J, Zorita E, Wagner S, *et al.* Influence of similarity measures on the performance of the analog method for downscaling daily precipitation. Clim Dyn. 2008; 30(2-3):133-44.
31. Manzanas R. Assessing the suitability of statistical downscaling approaches for seasonal forecasting in Senegal. Atmos Sci Lett. 2017; 18(9):381-6.
32. Mehran A, Aghakouchack A, Phillips TJ. Evaluation of CMIP5 continental precipitation simulations relative to satellite-based gauge-adjusted observations. J Geophys Res Atmos. 2014; 119:1695-707.
33. Miao C, Duan Q, Sun Q, Huang Y, Kong D, Yang T, *et al.* Assessment of CMIP5 climate models and projected temperature changes over Northern Eurasia. Environ Res Lett. 2014; 9(5):1-12.
34. Cubasch U, Wuebbles D, Chen D, Facchini MC, Frame D, Mahowald N, *et al.* Introduction in Climate Change. In: Stocker TF, Qin D, Plattner G-K, Tignor M, Allen S., Boschung J, *et al.*, (ed.). Intergovernmental Panel on Climate Change 2013: The Physical Science Basis Contribution of Working Group I to the Fifth Assessment Report of the Intergovernmental Panel on Climate Change. Cambridge. 2013; pp. 119-58.
35. Pierce DW, Barnett TP, Santer BD, Gleckler PJ. Selecting global climate models for regional climate change studies. Proc Natl Acad Sci. 2009; 106(21):8441-6.
36. Zubler EM, Fischer AM, Frob F, Liniger MA. Climate change signals of CMIP5 general circulation models over the Alps – impact of model selection. Int J Climatol. 2016; 36:3088-104.
37. Collins M, Knutti R, Arblaster J, Dufresne J., Fichefet T, Friedlingstein P, *et al.* Long-term Climate Change: Projections, Commitments and Irreversibility. In: Stocker T., Qin D, Plattner G., Tignor M, Allen S., Boschung J, *et al.*, (ed.). IPCC Fifth Assessment Report. Cambridge: Cambridge University Press. 2013; pp. 1029-136.
38. Tareghian R, Rasmussen PF. Statistical downscaling of precipitation using quantile regression. J Hydrol 2013; 487:122-35.

39. McSweeney C, New M, Lizcano G. UNDP Climate Change Country Profile: Zambia. School of Geography & Environment-University of Oxford & Tyndal Centre for Climate Change Research. 2008; 20:1-26.
40. Mpelele EB. Statistical Projections of Climate Change for Zambia Based on Simulations of Regional Climate Models. MSc in Statistics, Dissertation. University of Zambia, 2018.
41. IPCC. Summary for Policymakers. In : Climate Change 2013: The Physical Science Basis. Contribution of Working Group I to the Fifth Assessment Report of the Intergovernmental Panel on Climate Change. Stocker TF, Qin D, Plattner G-K, Tignor M, Allen SK, Boschung J, *et al*., editors. Cambridge, United Kingdom and New York, NY, USA.: Cambridge University Press, 2013.
42. IPCC. Climate Change 2014: Synthesis Report. Contribution of Working Groups I, II and III to the Fifth Assessment Report of the Intergovernmental Panel on Climate Change. Core Writing Team RKP and LAM, editor. Geneva, Switzerland: IPCC. 2014; pp. 151.
43. Josef D Daron. Regional Climate Messages for Southern Africa. 2014; pp.1-30.
44. Jain S. An empirical economic assessment of impacts of climate change on agriculture in Zambia. Policy Research Working Paper, 4291. World Bank, 2007.